Scientific Research Publishing

Journal of Geoscience and Environment Protection, 2026, 14(7), 414-426
https://www.scirp.org/journal/gep
ISSN Online: 2327-4344
ISSN Print: 2327-4336

Lg Waves Generated by the May 24, 2025 Earthquake in Borkou Region in Chad

Adoum Issak[1*], Doumnang Jean Claude[2], Mahamout Mahamat[3]

[1]Department of Physics, Faculty of Sciences and Technology, University of Doba, Doba, Chad
[2]Department of Geology, Faculty of Exact and Applied Sciences, University of de N'Djaména, N'Djamén, Chad
[3]Seismic Center of Abeche, University of N'Djaména, N'Djamén, Chad
Email: *iadoum961@gmail.com

How to cite this paper: Issak, A., Claude, D. J., & Mahamat, M. (2026). Lg Waves Generated by the May 24, 2025 Earthquake in Borkou Region in Chad. *Journal of Geoscience and Environment Protection, 14,* 414-426.
https://doi.org/10.4236/gep.2026.147023

Received: February 16, 2026
Accepted: July 26, 2026
Published: July 29, 2026

Abstract

This study follows the occurrence of an unexpected earthquake that occurred on May 24, 2025, in the Borkou region in the northern part of Chad. Chad is a stable zone in the tectonic point of view since it is located on a plate whereas earthquakes generally occur at the boundaries of plates, in subduction zones. The earthquake of May 24, 2025, with a magnitude 4.3 on the Richter scale, that occurred in this region is recorded and located at Chad station. The epicenter is located on a fracture line oriented SE-NW and passing through the South of Tibesti. The exploitation of data from the station before and after the event allowed us to conclude that it is an isolated earthquake, the kind often encountered in stable regions. The Lg waves that accompanied the earthquake were very well observed on a purely continental path and blocked on another path through the Mediterranean Sea. This is in perfect harmony with the mode of propagation of these waves which are blocked in an oceanic path.

Keywords

Earthquakes, Location, Borkou (Chad), Lg Waves

1. Introduction

The seismological station of Abéché located in eastern Chad operates in a small network of short-period sensors and one three-component sensor. The geographical position of the station in the heart of Africa allows it to record most seismic events occurring in the world. Comparative studies to assess the station's recording capacity were carried out from 1999 to 2003. These studies consisted of comparing the data from the Chad station with those from the REB bulletin (Review Event Bullen). The result for earthquakes of magnitude greater than or equal to 4 showed that approximately 80% of the teleseisms listed on the REB bullen are seen by the station in Chad, which reflects its high signal reception capacity. At the local level, the signals recorded are few in number and of very low magnitudes (on the order of 2 to 3), mostly from quarry shootings. The earthquake of May 2025 that occurred in the Borkou region (**Figure 1**) is the first of its kind to be felt by the population. The seismic calm that prevailed in the region after the earthquake shows that this is an isolated event. Although not destructive, the unexpected nature of the earthquake requires a thorough study to determine its real causes.

Figure 1. Map of Chad shown the Borkou Region.

2. Geological and Geophysical Context

The extract from the geological map of Chad (Schneider & Wolff, 1992) shows that the Chadian territory has mountainous areas distributed across the regions of Borkou, Ouaddaï, Wadi Fira, Guéra, and Mayo Kebi. These areas correspond to outcrops of Precambrian rocks. In the far north of the country lies the largest mountain range, the Tibesti, composed of a Precambrian basement covered by primary sandstone and then by tabular intercalated continental sandstone, all fractured and covered by Tertiary and Quaternary volcanic formations. The landscape features volcanoes such as Emi Koussi, which reaches 3415 m in altitude (the highest point in Chad), Pic Toussidé at 3315 m, and high plateaus called "Tarso" with altitudes between 2000 and 3000 m. The Emi Koussi volcano, whose last eruption is estimated to have occurred between 2.4 and 1.33 million years ago, remains an extinct volcano. To the northeast, one encounters Erdis, which are sandstone plateaus with ruin-like features, ranging in altitude from 500 to 800 meters. From a geophysical point of view, the studies in Chad started in 1954 with a team from ORSTOM. The team highlighted some large gravimetric routes (Grenn, 1955), and short online electrical soundings. The electrical and seismic refraction prospecting methods practiced by the General Geophysical Company (C.G.G), have been oriented towards the search for water. The gravimetry work carried out subsequently highlighted:

- the large trench that crosses all of southern Chad (Doba, Baké-Birao, Salamat) and which is located on the extension of the northern coast of the Gulf of Guinea.
- the large transversal Sao-Tome, Cameroon known as the "line of Cameroon" which would extend to Tibesti by a detour to the Erdis basin (Ounianga Kebir) (Fairhead, 1971; Cornacchia & Dars, 1983).

In seismology, research in Chad began with the exploitation of data from Abeche station since 2000. Since this period, no major earthquakes have been recorded in Chad. One can nevertheless note the existence of small signals of very low magnitudes, mostly from quarry shootings but also from natural earthquakes sometimes felt like the one in 2015 in the Waddifira region and 2021 in the Hadjer-lamis region.

3. Theoretical Background

Many studies have now been carried out in order to understand and interpret all the phases present on regional seismograms. Classically, we record the Pn, Pg, Sn, Sg and Lg phases (**Figure 2**). These phases are diffracted and refracted by the different heterogeneities they encounter along their propagation paths and thus form the secondary phases or the coda of the seismogram.

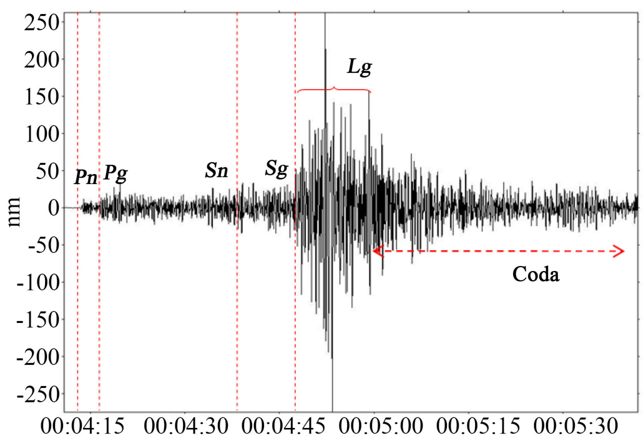

Figure 2. Sismogram of an earthquake in Sud Soudan located 300 km from station.

While classical wave trains are often well reproduced, the secondary phases that owe their existence to the heterogeneity of the propagation medium are generally more difficult to model (Bouchon, 1982). This difficulty comes on the one hand from the limited knowledge that we have of the propagation medium and on the other hand, from the misunderstanding that we have of the interactions between the wave field and the different heterogeneities of the medium. Indeed, although we now know relatively precisely the evolution of speed as a function of depth, lateral variations in speed are more difficult to assess. To this is added the difficulty of implementing digital techniques able to taking into account the threedimensional propagation effects of the wave field (Olsen et al., 1983).

A plane wave propagating through a seismological antenna is characterized by an oscillation frequency f_0 and a wave number vector:

$$s(r,t) = s_0 e^{i(\vec{k}_0 \vec{r} - 2\pi f_0 t)}$$

where So designates the amplitude of the signal, $\vec{k}_0$ is the wave vector that indicates the direction of wave propagation, f_0 is the signal frequency, and $\vec{r}(x,y,z)$ is the vector position.

The parameters of this wave field will be fully defined when we have known the frequency f_0 and the wave number k_0 that govern its propagation. One will then be able to estimate the direction of the wave which represents its azimuth θ_0 measured in degrees and its apparent propagation speed v_a.

$$\theta_0 = \text{arctg}\left(\frac{k_{\text{est}}}{k_{\text{nord}}}\right) \text{ and } v_a = \frac{2\pi f_0}{k_0}$$

The real velocity v of the wave is given by:

$$v = v_a \sin_0 .$$

4. Material and Method

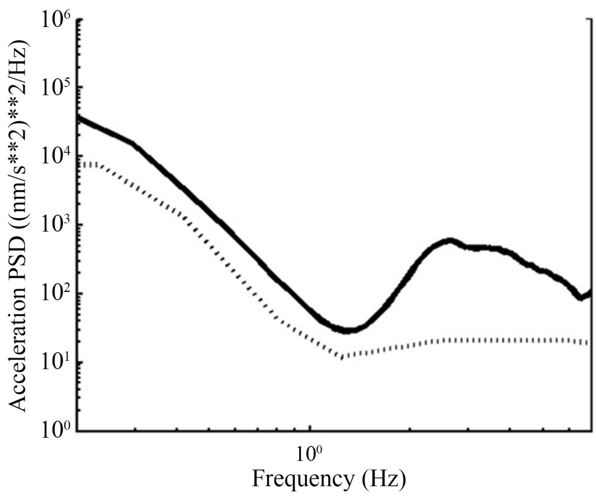

Figure 3. Average background noise of Chad station.

The Abeche station consists of a mini network of short-period sensors and a three-component sensor. The geometry of the mini-network consists of a succession of nested triangles suitable for locating seismic events at local, regional and telesismic distances. The short-period seismometers used are of the ZM500 type, sensitive to the vertical component of the seismic wave. The stations are located on well-rooted granite blocks, which ensures good coupling with the ground, good protection against atmospheric disturbances. In addition, their distance from the urban area and the sea allows to reduce as much as possible the background noise of industrial origin and the permanent effect of the marine swell that spreads over very long distances. Figure 3 is a comparison of the average background noise of the stations with the NLNM (New Low Noise Model) background noise model of Peterson (Peterson, 1993). This figure shows a good correlation with the model thus reflecting the quality of the signals recorded at the station. We see that between 0 and 1 Hz, all the stations have the same noise spectrum. This low-frequency noise is due to the combined action of the oceans and the atmosphere (oceanic swell). Beyond 1 Hertz, the local noise specific to each station is due to human activity and to the climatic environment.

5. Location of the Earthquake Studied

Figure 4 represents the signal trace in the three Components (ABC) and in the one component station (TIRE2) and Figure 5 represents the time-frequency distribution of seismic energies.

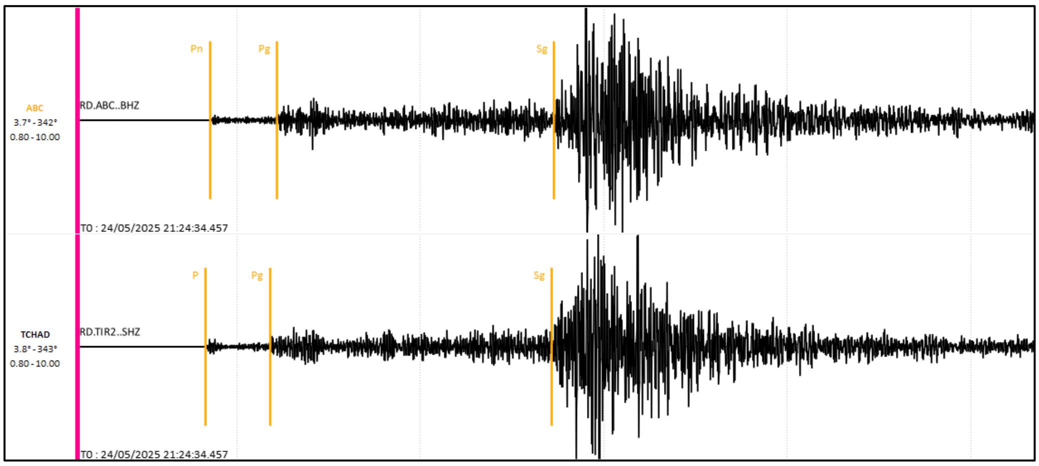

Figure 4. The signal recorded at ABC and TIRE stations: Z component.

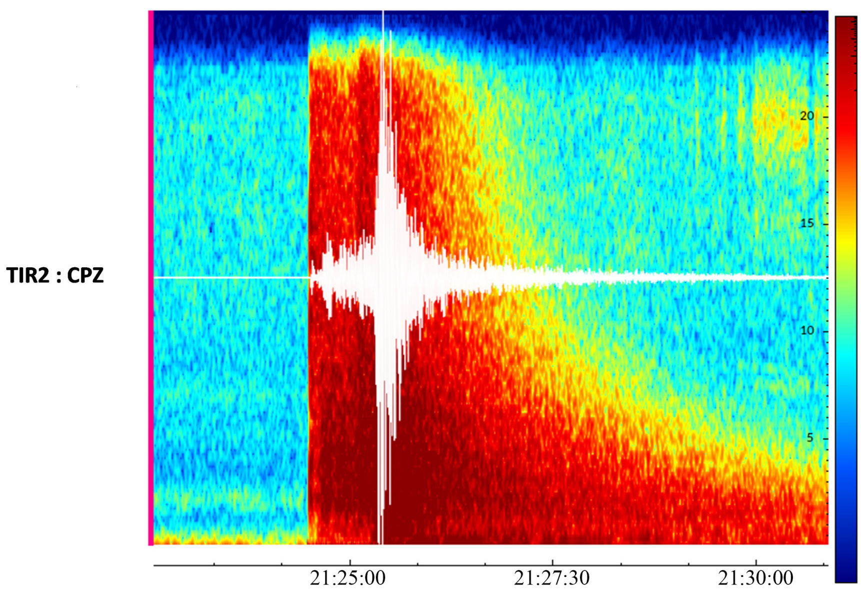

Figure 5. The time-frequency representation of the signal at T1R2 station.

We then calculated the polarization of the Pn, Pg and Sg waves recorded at station ABC.

The Waves polarization is estimated statistically from the data recorded by each of the North-South, East-West and vertical Z components (Jurkevics, 1998). For this, the covariance matrix of the data is constructed:

$$S_{jk} = \frac{XX^T}{N}\left[\frac{1}{N}\sum_{i=1}^{N} x_{ij} S_{ik}\right]$$

where x_{ij} is the ith component of the ground motion, N is the number of points used on each component. T is the transpose of the matrix X.

The x_{ij} covariance matrix is a real and symmetric 3 × 3 matrix whose main diagonal elements represent the self-covariance of the components and the other elements represent the cross-covariance; it is written:

$$S = \begin{pmatrix} S_{zz} & S_{zn} & S_{ze} \\ S_{zn} & S_{nn} & S_{ne} \\ S_{ze} & S_{ne} & S_{ee} \end{pmatrix}$$

The polarization ellipsoid is estimated by finding the main axes of the ellipsoid by calculating the eigenvalues and eigenvectors of S using the equation

$$\left(S - \lambda^2 I\right)u = 0$$

where I is the 3 × 3 identity matrix, and represent the eigenvalues and eigenvectors, respectively.

Then we determine:

In the horizontal plane, the azimuth of the wave by the north-south and east-west components:

$$Az(P) = \arctan\left(\frac{u_{21}\text{sign}(u_{11})}{u_{31}\text{sign}(u_{11})}\right)$$

The u_{ij} represent the director cosine of eigenvectors. The u_{ij} sign function is introduced to resolve the ambiguity of 180˚ by taking the positive vertical component.

In the vertical plane, the angle of incidence between the vertical and the horizontal plane:

$$i = \arccos\left|u_{11}\right|$$

Figure 6 represents the signals of Z, N and E components of the station ABC filtered in [0.5 - 4.0] Hz frequency band. On this figure, the red brackets represent the time range used for polarization computation of each phase. On the bottom, we have the waveform polarization in horizontal plane giving the back-azimuth for Pg wave (**Figure 7**), Pn wave (**Figure 8**) and Sg wave (**Figure 9**). The two P phases are polarized in longitudinal plane, and Sg wave is polarized in transverse plane. Yellow marker indicates theoretical back-azimuth and red arrow represents measured back-azimuth.

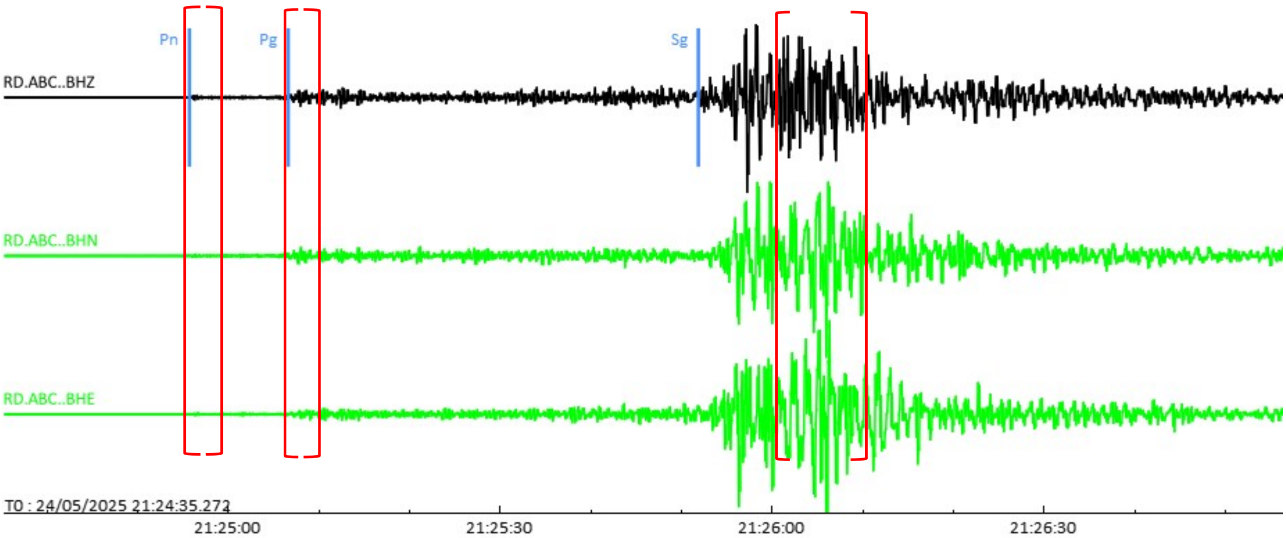

Figure 6. Signals of Z, N and E components of the station ABC.

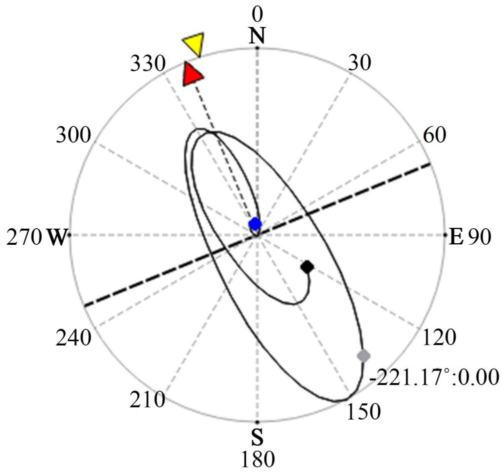

Figure 7. Polarization in horizontal plane giving the Azimut of Pg phase.

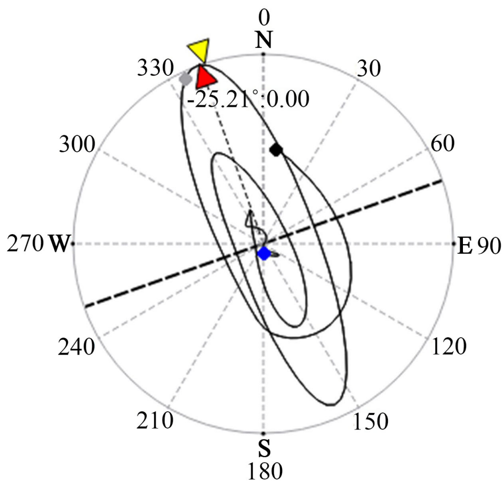

Figure 8. Polarization in horizontal plane giving the Azimut of Pn phase.

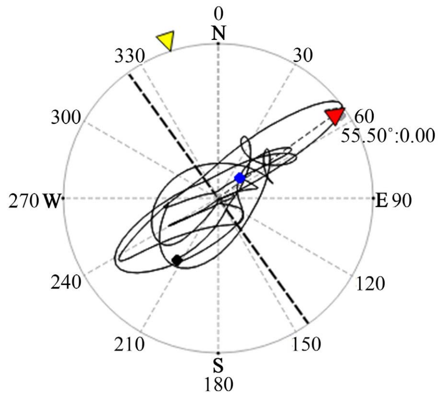

Figure 9. Polarization in vertical plane giving the Incidence angle of Sg phase.

Location settings

The localization is done in two steps: The first step consists to plot the arrival times at different stations. The second step consists of adjusting the parameters by hand, adjusting arrival times in order to obtain the best possible RMS. About the depth, this earthquake takes place in the upper part of the continental crust and therefore its depth is estimated between (2 - 3) km and (10 - 15) km. The localization is done by the ONYX software provided by the (LDG) Laboratory of Detection and Geophysics of Bruyères-Le-Châtel in Paris. The settings used in the localization software are listed in **Table 1** below.

Table 1. Calculation parameters.

Processing parameters	p-phase	Lg-phase
Frequency (Hz): Bandwidth	0.7 - 2.2	0.7 - 2.2
Filter order	2	2
Window duration	3s	10s
Shift	1	3
Sampling Frequency	50	50

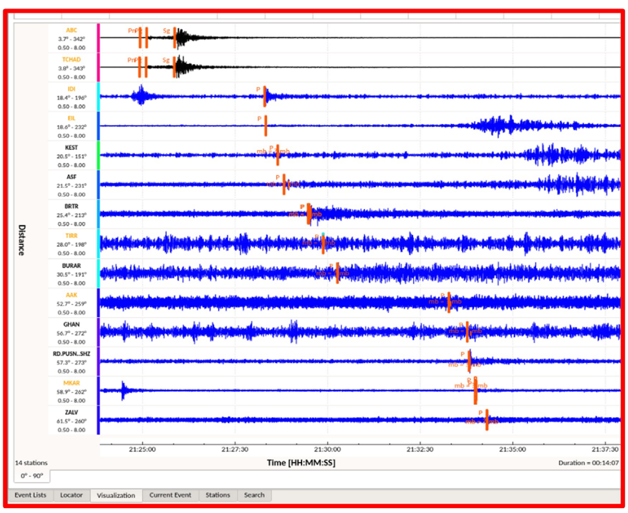

Figure 10. Arrival times at different stations.

Figure 10 shows the stations that contributed to the localization.

Only two stations in the Abéché array (TIR2 and ABC) have contributed to this location. The other stations are in the LDG network with which we collaborate. The result of the localization is summarized in Table 2 below:

Table 2. Location parameters.

Date	Time (UT)	Latitude	Longitude	Depth	Magnitude	Location ellipse			Time residual (rms)
						semi major axis	semi minor axis	azimuth	
2025-05-24	21:23:58.0	17.37N	19.68E	2 km	mb 4.3	25.7 km	6.9 km	86.0˚	2.1

6. Lg Waves

The Lg waves were first identified by Press and Press and Ewing (1952). They are interpreted on the one hand as resulting from the superposition of upper surface wave modes (Rayleigh and Love waves) propagating inside the continental crust and on the other hand being the envelope of S-waves reflected on the base of the crust and whose all energy has trapped within Oliver and Ewing (1957), Douglas (1990). Lg waves propagate mainly on continental paths. Their velocity is close to the average velocity of S-wave in the upper part of the continental crust. It's worth about 3.6 km/s. The earthquake studied have generated Lg waves recorded by two stations located in the north part of the Chad station. These are the IDL stations located beyond the Mediterranean and the EIL station located in Israel. Lg waves are very well observed on the EIL path while they are blocked on the IDL path that crossed the Mediterranean, Figure 11 and Figure 12. The Lg/P ratio is about 6 on the IDL patch, whereas this ratio is estimated at 1/10 on the EIL patch.

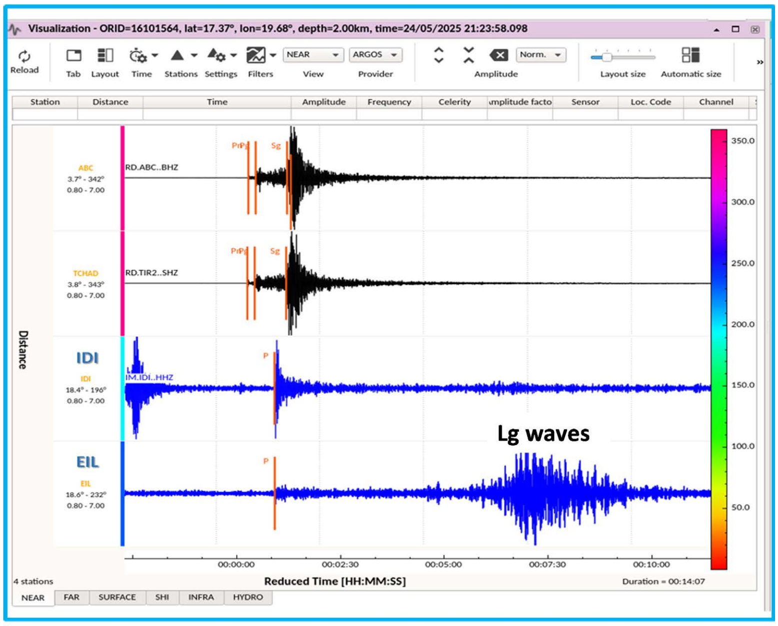

Figure 11. Lg waves recording.

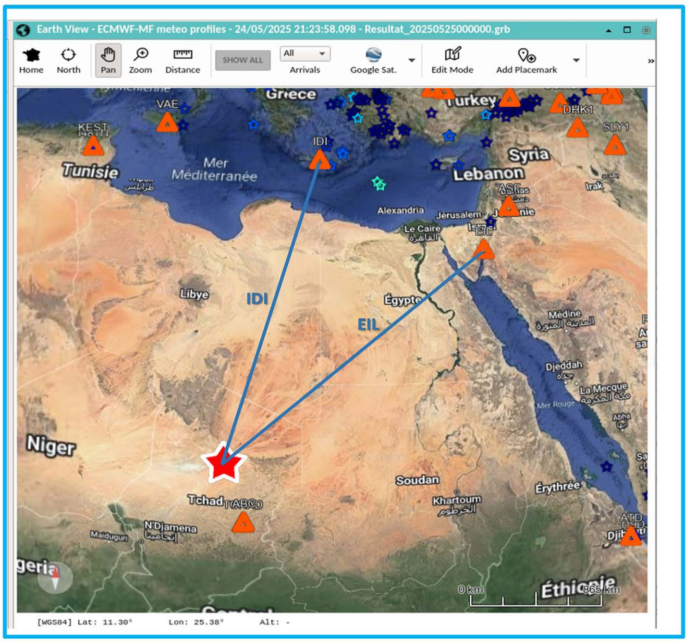

Figure 12. Path of Lg waves from the EIL and IDL stations.

7. Discussions

7.1. The POSSIBLE Causes of the Earthquake

Figure 13 represents the tectonic map of Africa seen from Chad. This figure shows breaks from the Jabel Mara in Sudan through the Tibesti. Figure 14 shows the location of the earthquake relative to the station (ABC). Figure 15 is an excerpt from the Borkou tectonic map on which the epicenter was plotted.

One can also notice from these figures that the earthquake is located on a fracture line, oriented SE-NW and passing through the south of the Tibesti (Guiraud et al., 2000) massif. This large lineament is a succession of faults that extend from the Great Lakes to the Hoggar crossing the Tibesti.

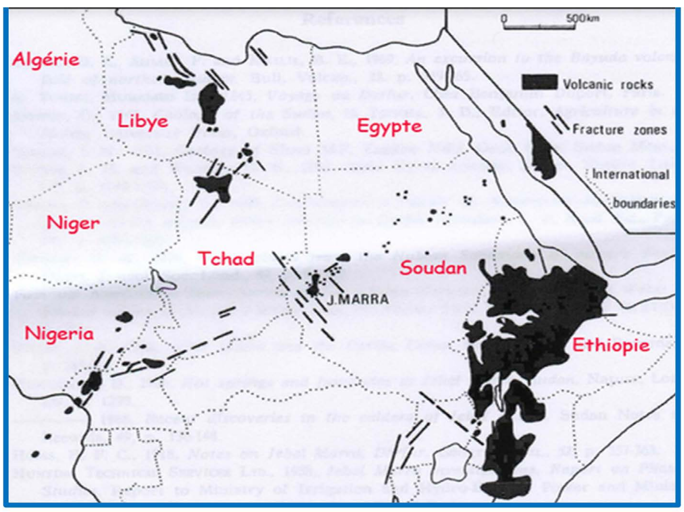

Figure 13. Tectonics of Africa and its boundaries.

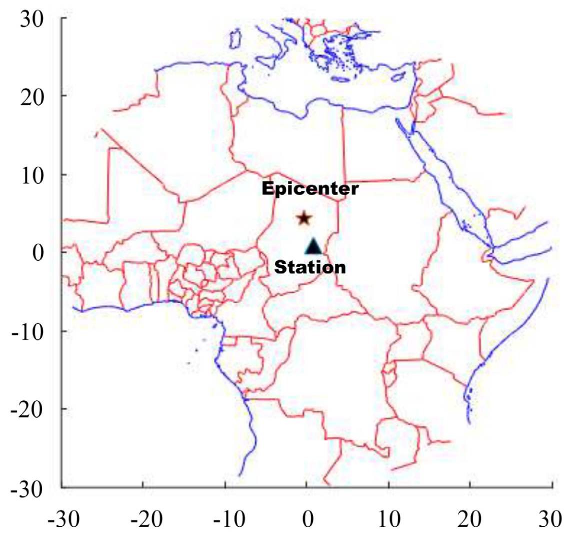

Figure 14. Location of the epicenter and station.

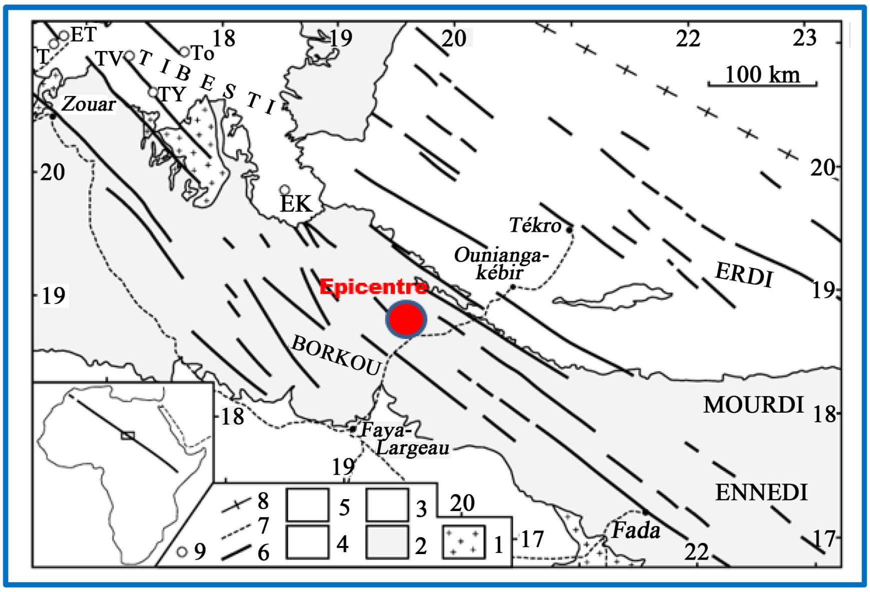

Figure 15. Location of the epicenter on the Borkou Tectonic map.

7.2. Lg Waves Blockage

The earthquake has generated Lg waves recorded on two sufficiently distant stations. At the EIL station, the path could be a continental crust in which the Lg waves propagate efficiently by multiple reflections on the base of the crust. At the IDL station, whose path crossed the Mediterranean Sea, the Lg waves are blocked. This show that the Mediterranean Sea has mainly an oceanic crust, that is to say thinner and of different composition than the continental crust. The extinction of Lg waves across the Mediterranean is due to the presence of this oceanic crust, which attenuates these waves. We notice that the Lg waves are not completely extinguished when crossing the Mediterranean. This is explained by a principle of conversion of Sn waves into Lg at the continental margin (Isacks & Stephens, 1975).

8. Conclusion

In the literature, we have not received any information on the occurrence of a major destructive earthquake in Chad. However, in recent years more or less significant earthquakes have been recorded, thus showing seismic activity in the in Chad. The current earthquake in the Borkou region is located on a fracture line highlighted by satellite, topographic and seismic data. This line consists of the spectacular lineaments on the edge of the mountain ranges oriented SE-NW and passing through the south of the Tibesti massif. This large lineament is the succession of faults that extend from the Great Lakes to the Hoggar crossing the Tibesti. These faults, locally observed in Algeria and Kenya, correspond to all the faults that have affected the Pan-African chains. They can replay and cause earthquakes. However, the non-reproducible nature of the event shows that it is an isolated earthquake, the kind we encounter but not often in stable continental regions (Calais et al., 2016). The homogeneity of the continental crust made it possible to record Lg waves at station EIL located at a very long distance. On the other hand, these waves are blocked on the path that crossed the Mediterranean. This observation is in perfect agreement with the mode of propagation of Lg waves which are strongly attenuated by an oceanic crust. Indeed, the station in Chad has been operating since 2012 and from then until today, only three significant earthquakes have been recorded in Chad: on June 23, 2015 in northeastern Chad, on March 20, 2021 in the Hadjer Lamis, and on May 25, 2025 in Borkou.

Conflicts of Interest

The authors declare no conflicts of interest regarding the publication of this paper.

References

Bouchon, M. (1982). The Complete Synthesis of Seismic Crustal Phases at Regional Distances. *Journal of Geophysical Research: Solid Earth, 87,* 1735-1741. https://doi.org/10.1029/jb087ib03p01735

Calais, E., Camelbeeck, T., Stein, S. M. et al. (2016). A New Paradigm for Large Earthquakes in Stable Continental Plate Interiors. *Geophysical Research Letters, 43,* 621-637.

Cornacchia, M., & Dars, R. (1983). Un trait structural majeur du continent Africain; les lineaments centrafricains du Cameroun au Golfe d'Aden. *Bulletin de la Société Géologique de France, 7,* 101-109. https://doi.org/10.2113/gssgfbull.s7-xxv.1.101

Douglas, R. B. (1990). Investigation of Tele-Seismic LG Blockage and Scattering Using Regional Arrays. *Bulletin of the Seismological Society of America, 80,* 2261-2281.

Fairhead, J. D. (1971). The Seismicity of Africa. *Geophysical Journal International, 24,* 271-301. https://doi.org/10.1111/j.1365-246x.1971.tb02178.x

Grenn, Y. (1955). *Anomalies de la pesanteur au Tchad.* O.R.S.T.O.M., 20 p.

Guiraud, R., Doumnang Mbaigane, J. C., Carretier, S., & Dominguez, S. (2000). Evidence for a 6000 km Length NW-SE-Striking Lineament in Northern Africa: The Tibesti Line-

ament. *Journal of the Geological Society, 157,* 897-900.
https://doi.org/10.1144/jgs.157.5.897

Isacks, B. L., & Stephens, C. (1975). Conversion of Sn to Lg at a Continental Margin. *Bulletin of the Seismological Society of America, 65,* 235-244.
https://doi.org/10.1785/bssa0650010235

Jurkevics, A. (1998). Polarization Analysis of Three-Component Array Data. *Bulletin of the Seismological Society of America, 78,* 1725-1743.

Oliver, J., & Ewing, M. (1957). Higher Modes of Continental Rayleigh Waves. *Bulletin of the Seismological Society of America, 47,* 187-204.
https://doi.org/10.1785/bssa0470030187

Olsen, K. H., Braile, L. W., & Stewart, J. N. (1983). Modeling Short-Period Crustal Phases (P-Lg) for Long-Range Refraction Profiles. *Physics of the Earth and Planetary Interiors, 31,* 334-347. https://doi.org/10.1016/0031-9201(83)90093-6

Peterson, J. (1993). *Observations and Modeling of Seismic Background Noise* (95 p). U.S.G.S., Open File Report.

Press, F., & Ewing, M. (1952). Two Slow Surface Waves across North America. *Bulletin of the Seismological Society of America, 42,* 219-228.
https://doi.org/10.1785/bssa0420030219

Schneider, J. L., & Wolff, J. P. (1992). *Geological and Hydrogeological Map at 1/1,500,000 of the Republic of Chad*. Explanatory Memorandum, BRGM Document No. 209.